

## Characterization of Protein-Based Complexes loaded with anthocyanins from Purple Sweet Potato

Mauricio E. Martinon<sup>2</sup>, M. Elena Castell-Perez<sup>1\*</sup>, Zeynep Sevimli-Yurttas<sup>2</sup>, Rosana G. Moreira<sup>2</sup>

<sup>1</sup>Department of Biological and Agricultural Engineering, Texas A&M University, College Station, USA

<sup>2</sup>Department of Biological and Agricultural Engineering, Texas A&M University

\*Corresponding Author: M. Elena Castell-Perez, Department of Biological and Agricultural Engineering, Texas A&M University, College Station, USA, Email: ecastell@tamu.edu

### ABSTRACT

The functional characteristics of protein-based complexes for use as carrier systems of Purple Sweet Potato (PSP) Anthocyanins (ACN) were evaluated using rheological, physical and microscopy principles. Four different concentrations of PSP-ACN stock solution (2, 5, 15, and 25 mg) were mixed with 20  $\mu$ M of protein in NaCl solution (final mix concentration) from three different types of protein: soy protein isolate (SPI, 90% protein), whey protein isolate (WPI, 90-92% protein), and  $\alpha$ -Lactalbumin ( $\alpha$ -L, 90%). Stability at two pH 1.35 and 7.45 was also evaluated. Dynamic oscillatory tests on dilute biopolymer solutions were performed at 23°C to determine the relaxation time ( $\lambda$ ) and a critical frequency value (CFV) to characterize the structure of the protein-based complexes and explain why some proteins yield more stable and efficient matrices. Higher concentrations of PSP-ACN yielded lower CFVs and this trend was more significant ( $P < 0.05$ ) for the WPI samples. The SPI complexes produced smaller structures at the 5-25 mg/L concentration levels (lower CFV values) which were also more sensitive to shear –i.e., frequency. Transmission Electron Microscopy (TEM) was carried out to observe distribution and size of the particles within the protein matrix. These observations correlated well with the entrapment efficiency (EE %) and loading capacity (%LC) of the complexes. The  $\alpha$ -Lactalbumin samples had higher entrapment efficiency, loading capacity, and PSP-ACN to protein ratios while the soy protein isolate (SPI) complexes yielded the lowest ratios at all concentrations, mainly due to the amount of electrostatically precipitated protein remaining constant and unaffected by changes in the PSP-CAN concentration. The increase in EE% with increasing PSP-ACN concentration resulted in better entrapment ratios for WPI and  $\alpha$ -L but not for SPI. Results provide new knowledge on the functional and rheological properties of selected protein-based complexes for use as effective purple sweet potato anthocyanin carriers.

**Keywords:** rheology; microscopy; encapsulation; structure; stress relaxation; biopolymer; antioxidants; critical frequency value

### INTRODUCTION

Development of value-added health foods using purple sweet potato (PSP) is popular because of the higher concentration of anthocyanins per kilogram of potato compared to other sources (84-174 mg/100g) (Bovell-Benjamin, 2007; Sudaet al., 2008; Bridgers, Chin & Van-den, 2010; Ray, Panda, Swain & Sivakumar, 2012; Li et al., 2019). Anthocyanins (ACN) are the most important class of water-soluble pigments responsible for red to blue colors in various plants with excellent antioxidant properties (He & Giusti, 2010; Oidtmann et al., 2012; Pojer, Johnson & Stockley, 2013).

Functional food products should not only provide a significant dose of such bioactive

molecules, but these molecules must also remain fully functional for as long as needed (Garti, 2008; Fernandes, de Freitas & Mateus, 2014). Because anthocyanins are thermolabile compounds, efficient delivery methods that would both carry and protect the bioactive compounds have been investigated (Parada & Aguilera, 2007; Crowe, 2013).

Structurally-designed matrices may assist in delivering the bioactive compound to the intended site of action within the body. For example, in some foods, polyphenols exist as conjugates with proteins resulting in soluble and insoluble protein-polyphenol complexes that have a stabilizing effect on polyphenols. Although, protein-rich ingredients have been investigated for their potential to bind anthocyanins and

increase their stability in developed functional foods (Gunasekaran, Ko & Xiao, 2007; Parada & Aguilera, 2007; Ahmed, Akter, Lee&Eun, 2010; Crowe, 2013; Peng, Li, Guan & Zhao, 2013; Ribnicky et al., 2014; Padzil, Aziz & Muhamad, 2019), there is still need for the characterization of molecular complexes (assemblies) using physical methods such as rheology (Woodward, Kroon, Cassidy & Kay, 2009; Kamonpatanaet al., 2012; Liu et al., 2014, 2015; Lu et al., 2015; Puerta-Gomez and Castell -Perez, 2016).

The flow characteristics or rheological behavior of polymeric compounds in diluted solution are extremely sensitive to the structure of the molecules thus affecting their functionality (Chamberlain and Rao, 2000). Dynamic oscillatory tests may be used to provide critical information about the structure and the type of association presented by these biopolymers by characterizing their Viscoelastic behavior. The viscoelasticity of polymeric composites is described by the relationship between their solid/elastic ( $G'$ ) and fluid/viscous ( $G''$ ) moduli through a relaxation time,  $\lambda$ -value, spectrum (Utracki, 2004; Sunthar, 2010; Puerta-Gomez and Castell-Perez, 2016). This relaxation time and its decrease up to a critical frequency value (CFV) in an oscillatory test have been linked to the structure and stability of polymeric compounds (Chhabra, 2010; Puerta-Gomez and Castell-Perez, 2016). If highly elastic (high  $G'$  values), polymers in dilute solutions can overcome proportional stresses and strains without disrupting the integrity of the network structure. If highly viscous (high  $G''$  values), the structure is weak and easily disrupted (Osaki, Inoue, and Uematsu, 2001; Schramm, 2002; Puerta-Gomez and Castell-Perez, 2016).

This study evaluated the functional and rheological characteristics of protein-based complexes as potential delivery systems for PSP-ACN by quantifying the intrinsic characteristics of the protein-based carriers using rheological, physical and microscopy principles; while also determining its stability under different pH conditions.

## MATERIALS AND METHOD

### Anthocyanin (ACN) Isolation

Purple sweet potato extract (*Dioscoreaalata*) was obtained from Avoca Inc. (Merry Hill, NC), and anthocyanin(ACN) isolated by partitioning from a 10g reversed phase Sep-Pak C18 20 cc cartridge (Waters Corporation, Milford, MA) that was previously conditioned with methanol and rinsed with deionized water to remove any

polar constituents. Next, ethyl acetate was added to elute the majority of phenolic acids and flavonoids and PSP-CAN recovered with acidified methanol (0.01% HCl), concentrated following solvent evaporation under vacuum at 30°C, and stored at 4°C until further analysis (Pacheco-Palencia, & Talcott, 2007). Concentrated PSP-ACN were standardized to a stock concentration in terms of mg of Cyanidin-3-Glucoside (C3G) equivalents/L using the Wrolstad's pH differential method of Wrolstad (2002). The anthocyanins monomeric pigment concentration (MAC) in the original samples was obtained using Eq. (1) and assuming a path length  $l$ , of 1cm:

$$MAC (mg/L) = (A \times Mw \times D_f \times 1000) / (\epsilon \times l) \quad (1)$$

where  $Mw$  is the molecular weight,  $A$  is the absorbance,  $D_f$  is the dilution factor, and  $\epsilon$  is the molar absorptivity. Cyanidin 3-glucoside (C3G) is used as the reference pigment with a  $Mw = 449.2$  g/mol and  $\epsilon = 26,900$  ( $10^6$  L/mol cm). The absorbance of the diluted sample ( $A$ ) was calculated as:

$$A = (A_{\lambda_{vis-max}} - A_{700})_{pH=1.0} - (A_{\lambda_{vis-max}} - A_{700})_{pH=4.5} \quad (2)$$

### Sample Preparation

The procedure followed in this study was adapted from the method published by our lab (Puerta-Gomez and Castell-Perez, 2015). Briefly, four different concentrations of PSP- ACN stock solution (2, 5, 15, and 25 mg) were mixed with 20  $\mu$ M of protein (total biopolymer amount of 184 g/L, 18.4% wt. ratio) in NaCl solution (final mix concentration) from three different types of protein: soy protein isolate (SPI, 90% protein, Archer Daniels Midland Co., Decatur, IL), whey protein isolate (WPI, 90-92% protein), and  $\alpha$ -Lactalbumin ( $\alpha$ -L, 90%), both from DAVISCO Foods International, Inc., Eden Prairie, MN. Afterwards, samples were subjected to two cycles of sonication at 42 KHz for 10 minutes (Branson Ultrasonic Corp. Danbury, CT), vortex mixed for 60 seconds, and subsequently stored at 4°C overnight. The following day the samples were kept at 23°C for 2 hr prior to performing the rheological tests. Particles were then synthesized by acid precipitation of ACN-Protein complexes in order to conduct the rest of the experiments.

### Particle Synthesis by Electrostatic Precipitation of Proteins

Among the different techniques to encapsulate bioactive compounds by protein aggregation,

only electrostatic precipitation of protein is a reversible process that does not involve significant change on the protein native structure (Puerta-Gomez & Castell-Perez, 2016). Upon homogenization and blending of PSP-ACN and protein, the solution was precipitated by addition of citrate buffer (1 M) to achieve the isoelectric point of the proteins (pH ~4.5) involved in the particle complex. After that the sample was placed into four 45 ml centrifuge tubes and let to rest for 30 minutes, the solution was then centrifuged (Allegra 25R centrifuge, Beckman Coulter, Fullerton, CA) at 4°C for 20 minutes and the liquid supernatant was separated for further quantification of non-entrapped PSP-ACN content. After centrifugation, the precipitate was kept at -20°C overnight and then lyophilized at -50°C and 1.45 × 10<sup>-4</sup> psi vacuum for 12 h in a Labconco Freeze Dry- 5 unit (Labconco, Kansas City, MO). Afterwards, the particles were stored at -20°C until further analysis.

### Entrapment Efficiency and Loading Capacity

The entrapment capability of the complexes was evaluated by measuring the remaining amount of PSP-ACN present on the supernatant after centrifugation and calculated as:

$$\text{Entrapment Efficiency } \% = \frac{(ACN_{control} - ACN_{supernatant})}{ACN_{control}} \times 100 \quad (3)$$

A control PSP-ACN solution was prepared with the absence of protein to serve as reference. To quantify the amount of PSP-ACN, a 100 µl-sample was diluted 20 times with acidified methanol (0.01% HCl) and passed through 0.2 µm nylon membrane syringe filters (VWR Intl., West Chester, PA) to remove all protein complexes precipitated on methanol. The filtered solution was assessed through absorbance (Abs) measurements using a spectrophotometer (Shimadzu UV-1601 spectrophotometer, Columbia, MA) at 530 nm in a 1 cm path length quartz cuvette. The amount of total PSP-ACN was calculated in mg/L of C3G equivalents using an extinction coefficient of 34,300 (Giusti & Wrolstad, 2001). Upon electrostatic precipitation and lyophilization of the samples, the weight of the dry sediment was recorded to calculate the concentration of mg PSP-ACN per gram of protein. The loading capacity (LC%) was calculated as

$$\text{Loading capacity } \% = \frac{(ACN_{control} - ACN_{supernatant})}{\text{weight of nanoparticle}} \times 100 \quad (4)$$

### Particle Characterization Using Rheological Analysis

Rheological tests were performed with a Haake Rheo Stress 6000 Rheometer (Thermo Fisher Scientific, Waltham, MA) with a cone-plate geometry (60 mm in diameter and angle of 1 degree with a gap of 0.052 mm). This geometry was selected because the shear rate within the gap is constant. 1 mL of sample was placed in the bottom plate for 5 minutes to allow for structure recovery. The sample temperature was maintained at 23°C with a TC-81 Peltier system (Thermo Fisher Scientific, Waltham, MA). A stress sweep was performed to determine the region where the moduli (G' and G'') are constant, known as the linear viscoelastic region or LVR. Next, small amplitude oscillatory angular frequency (ω) sweeps (from 0.01 to 1000 rad/s) were performed at a stress of 0.01 Pa for the WPI and ω-L dilute solutions, and at a stress of 0.1 Pa for the SPI solutions. This difference in LVR is linked to the SPI's ability to yield higher amounts of sediment upon electrostatic precipitation, therefore resulting in a higher LVR stress value. The dynamic response (G' and G'' as a function of frequency or mechanical spectra) was used to characterize the Viscoelastic behavior of the solutions containing PSP-ACN-protein compounds

The stability of PSP-ACN-protein structures was characterized by evaluating the relaxation time λ [s/rad] associated with changes in the structure of the particles at a critical frequency value (CFV) as (Schramm, 2002; Roland, 2008; Puerta-Gomez et al., 2016):

$$\lambda = \frac{G'}{G'' \omega} \quad (5)$$

Changes in the slope of the λ-value versus frequency data are related to changes in structure and the CFV is equivalent to the maximum shear rate under which the PSP-ACN-protein complex will maintain its 3D conformation. Hence, the higher CFV, the more stable the structure. (Puerta-Gomez and Castell-Perez, 2016).

### Morphological Analysis

Aqueous suspensions of electrostatically precipitated PSP-ACN-Protein compounds were examined using a FEI Morgagni Transmission Electron Microscope (TEM) (FEI Company, Hillsboro, OR). The suspensions of particles were placed on 300 mesh copper grids and stained with a 2% (w/v) uranyl acetate aqueous stain (Electron Microscopy Sciences, Hatfield,

PA) to provide contrast under magnification. Excess liquid on the mesh was removed with filter paper and the grid was allowed to dry before viewing under 50,000-100,000 times magnification. Observations were performed at 80 kV.

### Particle Size Distribution

Particle size analysis was carried out using a LS 13 320 multi-wave length laser diffraction particle size analyzer (Beckman Coulter Inc., Miami, FL) which uses the theory of Mie scattering, Fraunhofer diffraction and Polarization Intensity Diffraction Scattering (PIDS). The method measures the size distribution of particles suspended in dry powder form and the particle sizerange of 0.375µm to 2000 µm. 5 grams of freeze dried compound wereplaced in the sample holder and analyzed for particle size distribution. Particle size characteristics (mean, median, mode, stdv) were computed automatically by the instrument and the median value (D50) was reported as compared to mean value.

### In Vitro Release Study

*In vitro* release studies of anthocyanin particles were carried out to determine the effect of pH on the release of the entrapped compound using a direct dispersion method (Jain & Jain 2010; Pulicharla, Marques, Das, Rouissi& Brar, 2016). The procedure was performed in two different mediums at pH = 1.35 and at pH = 7.45. The first solution consisted of a mixture of hydrochloric acid, potassium chloride, and water; while phosphate buffered saline solution was used as the second medium. Both solutions were then standardized to reach their respective pH (Chotiko&Sativel, 2017).

Entrapped anthocyanin (at the highest concentration, 25 mg/L) was dispersed in 30 ml of solution and incubated in a water bath shaker (VWR International 89032-226, West Chester, PA) at 35°C ± 0.5°C, 120 rpm for 24 hours. At pre-determined time intervals (20 min, 40 min,

60 min, 2, 4, 6, 8, 10, 12, and 24 hours), 1.5 ml of aliquots were withdrawn followed by replacement of the withdrawn volume by fresh buffer solutions to operate release studies under sink conditions. The withdrawn aliquots were centrifuged in a VWR Clinical 200 centrifuge (VWR Intl., West Chester, PA) at 3000 rcf for 10 min and the supernatant was then filtered through 0.2 µm nylon membrane syringe filters (VWR Intl., West Chester, PA) to remove all protein complexes precipitated. The filtered supernatant was monitored using a spectrophotomer (Shimadzu UV-1601 spectrophotometer, Columbia, MA) at 530 nm in a 1 cm path length quartz cuvette and the percentage of total PSP-ACN was calculated using a control sample consisting of unentrapped anthocyanin at the same concentration. The percentage of anthocyanin release was determined as:

$$\% AnthocyaninReleased = \frac{(C_t)}{C_0} \times 100 \quad (6)$$

where C<sub>0</sub> is the total amount of anthocyanin entrapped and C<sub>t</sub> represents the amount of anthocyanin released at a time t. All results were expressed as the mean standard error of three measurements performed at the time of the test. This method was chosen due to its simplicity and low cost to describe the release kinetics of the PSP-ACN loaded in protein-based capsules using SigmaPlot software (SigmaPlot, 2019.)

### Statistical Analysis

All experiments were carried out in triplicate unless reported otherwise, and the results were reported as average. Statistical analysis software (IBM SPSS Statistics, Version 25 IBM Corporation, Armonk, NY) was used to perform analysis of variance (ANOVA) in a general linear model. Mean comparison analysis were performed with the Tukey test (Dunnett T3 for unequal variances) to compare differences in entrapment efficiencies among the ACN-Protein samples with a P < 0.05 being considered to be a significant difference between means.

**Table1.** Entrapment efficiency (EE%) and average loading capacity (LC %) as a function of concentration of purple sweet potato anthocyanin (PSP- ACN) encapsulated with different proteins

Protein <sup>1</sup>	PSP- ACN concentration (mg/L)			
	2	5	15	25
EE%				
WPI	<sub>x</sub> 67.74 <sup>a</sup> (2.794) <sup>*</sup>	<sub>y</sub> 87.88 <sup>b</sup> (1.312)	<sub>x</sub> 89.69 <sup>b</sup> (4.460)	<sub>x</sub> 95.56 <sup>c</sup> (2.151)
□-L	<sub>x</sub> 91.93 <sup>a</sup> (2.794)	<sub>z</sub> 94.69 <sup>a,b</sup> (1.312)	<sub>x</sub> 93.99 <sup>a,b</sup> (1.966)	<sub>x</sub> 97.29 <sup>c</sup> (0.938)

## Characterization of Protein-Based Complexes loaded with anthocyanins from Purple Sweet Potato

SPI	$\bar{x}$ 75.80 <sup>a</sup> (14.516)	$\bar{x}$ 82.58 <sup>a,b</sup> (1.312)	$\bar{x}$ 94.42 <sup>a,b</sup> (3.240)	$\bar{x}$ 97.01 <sup>b</sup> (2.483)
<b>LC%</b>				
WPI	$\bar{x}$ 11.97 <sup>a</sup> (0.005)	$\bar{x}$ 14.76 <sup>b</sup> (0.020)	$\bar{x}$ 14.181 <sup>b</sup> (0.007)	$\bar{x}$ 16.08 <sup>b</sup> (0.0041)
□-L	$\bar{y}$ 20.65 <sup>ab</sup> (0.006)	$\bar{x}$ 19.94 <sup>b</sup> (0.003)	$\bar{x}$ 15.13 <sup>a</sup> (0.003)	$\bar{x}$ 17.03 <sup>a</sup> (0.002)
SPI	$\bar{z}$ 4.75 <sup>ab</sup> (0.006)	$\bar{z}$ 5.00 <sup>a</sup> (0.001)	$\bar{y}$ 6.07 <sup>ab</sup> (0.002)	$\bar{y}$ 5.74 <sup>b</sup> (0.001)

<sup>1</sup> WPI = whey protein isolate; □-L = alpha lactalbumin; SPI = soy protein isolate, \*Values represent mean  $\pm$  standard deviation of three replicates per sample, <sup>a,b,c</sup> Mean values with a different superscript letter in a row are significantly different than the others ( $p < 0.05$ ), <sup>x,y,z</sup> Mean values with a different subscript letter in a column are significantly different than the others ( $p < 0.05$ ).

## RESULTS AND DISCUSSION

### Entrapment Efficiency and Average Loading Capacity

The higher the PSP-ACN concentration, the higher the entrapment efficiency for all three PSP-ACN-protein complexes. Similarly, the loading capacity increased with increasing PSP-ACN concentration (Table 1). The EE% of the 5 mg/L PSP-ACN-□-L samples was higher ( $P < 0.05$ ) and varied within a smaller range (from 91.93% to 97.29%) than for the other proteins, suggesting a higher ability of □-L to entrap the anthocyanin even at the lower PSP-ACN concentrations. The type of protein affected ( $P > 0.05$ ) the loading capacity with the SPI samples

having lower LC% ( $P < 0.05$ ). Similarly, the □-L samples yielded higher PSP-ACN-protein ratios while the SPI complexes yielded the lowest ratios at all concentrations, because the amount of electrostatically precipitated protein remains constant. The PSP-ACN-protein ratios increase up to four times with concentration raising from 2 mg/L to 25 mg/L for WPI and □-L complexes (Table 2).

The increase in EE% with increasing PSP-ACN concentration resulted in better entrapment ratios for WPI and □-L. In practice, larger amounts of SPI would be needed to achieve the same level of entrapment efficiency than for the WPI and □-L systems.

**Table 2.** PSP- ACN protein ratios (mg ACN/g protein)

Protein <sup>1</sup>	PSP- ACN Concentration (mg/L)			
	2	5	15	25
WPI	$\bar{x}$ 0.239 <sup>a</sup> (0.001)*	$\bar{x}$ 0.738 <sup>b</sup> (0.011)	$\bar{x}$ 2.126 <sup>c</sup> (0.106)	$\bar{x}$ 4.019 <sup>d</sup> (0.089)
□-L	$\bar{y}$ 0.413 <sup>a</sup> (0.013)	$\bar{y}$ 0.997 <sup>b</sup> (0.014)	$\bar{x}$ 2.270 <sup>c</sup> (0.047)	$\bar{x}$ 4.258 <sup>d</sup> (0.041)
SPI	$\bar{x}$ 0.095 <sup>a</sup> (0.012)	$\bar{z}$ 0.250 <sup>b</sup> (0.004)	$\bar{x}$ 0.910 <sup>c</sup> (0.031)	$\bar{x}$ 1.436 <sup>d</sup> (0.037)

<sup>1</sup> WPI = whey protein isolate; □-L = alpha lactalbumin; SPI = soy protein isolate, \*Values represent mean  $\pm$  standard deviation of three replicates per sample, <sup>a,b,c</sup> Mean values with a different superscript letter in a row are significantly different than the others ( $p < 0.05$ ), <sup>x,y,z</sup> Mean values with a different subscript letter in a column are significantly different than the others ( $p < 0.05$ ).

### Mechanical Spectra of PSP-ACN Solutions under Oscillatory Frequency Sweeps

#### Effect of Protein Type on Viscoelastic Properties of Complexes

Figure 1 shows the mechanical spectra of the WPI and SPI samples (the ones for □-L solutions were similar but not shown). WPI and □-L samples showed typical dilute solution behavior with both proteins yielding similar spectra at all PSP-CAN concentration levels --larger  $G'$  values ( $P < 0.05$ ) at the lower frequencies, then both moduli

approaching and then crossing at the higher frequencies.

On the other hand, SPI yielded typical gel-like behavior with  $G'$  higher ( $P < 0.05$ ) than  $G''$  throughout the frequency range, for all PSP-ACN concentrations. These findings correlate well with the lower ( $P < 0.05$ ) ACN-protein ratios of the SPI complexes (more gel-like, higher elastic modulus  $G'$ ) compared to the more fluid-like behavior (higher  $G''$ ) of the other protein-based complexes at all the concentration levels evaluated in this study.

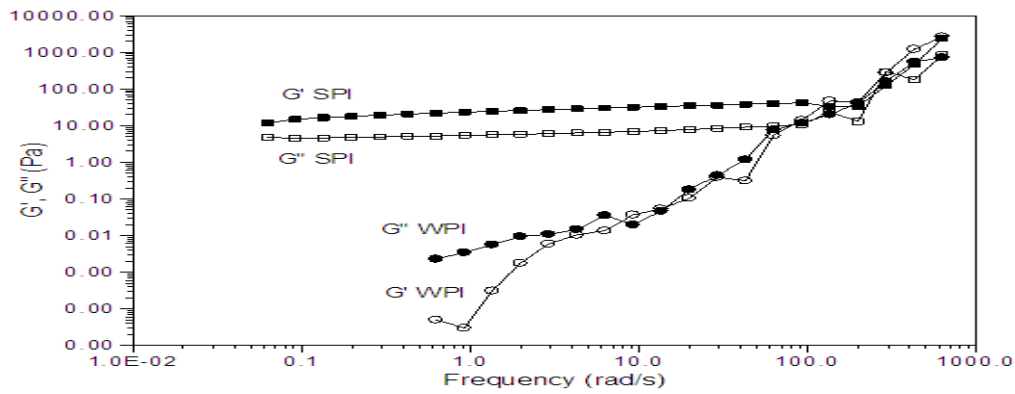


**Figure1.** Effect of protein type on the mechanical spectra of PSP-ACN-protein solutions (25 mg/L PSP- ACN concentration). Data obtained from frequency sweep at 23oC. LVR was established at 0.01 Pa and 0.1 Pa for WPI (whey protein isolate) and SPI (soy protein isolate), respectively. Spectra for □-lactalbumin were similar to that for WPI solutions at all concentrations (data not shown).

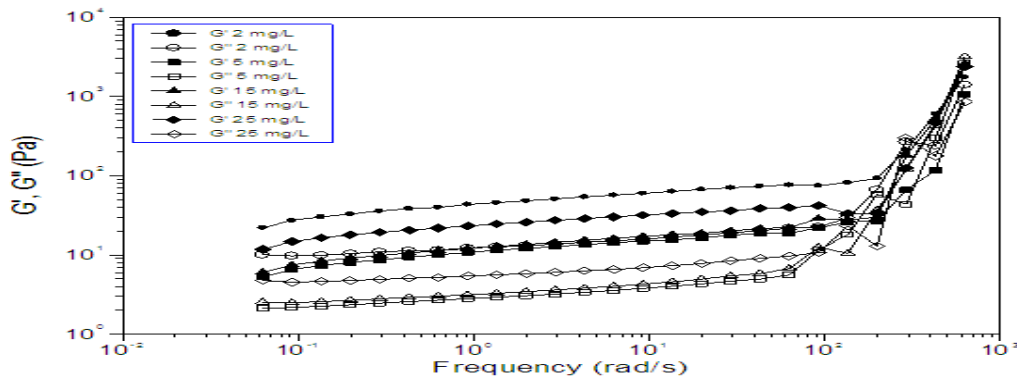


**Figure2.** Effect of PSP- ACN concentration on the mechanical spectra for PSP-ACN-SPI solutions. Data obtained from frequency sweep at 23oC. LVR was established at 0.1 Pa

**Effect of PSP-ACN Concentration on Viscoelastic Properties of Complexes**

The SPI-based complexes were used to illustrate the effect of PSP-CAN concentration on the mechanical spectra of the solutions (Figure 2). In general, the higher PSP-ACN concentrations yielded weaker gel-like materials (lower G' and

G'' values along the frequency spectrum) with some variability among the samples, suggesting the occurrence of some interaction between the anthocyanins and the protein which weakened the structure. This observation correlates with the lower EE%, LC%, and PSP-ACN-protein ratios for the SPI samples.

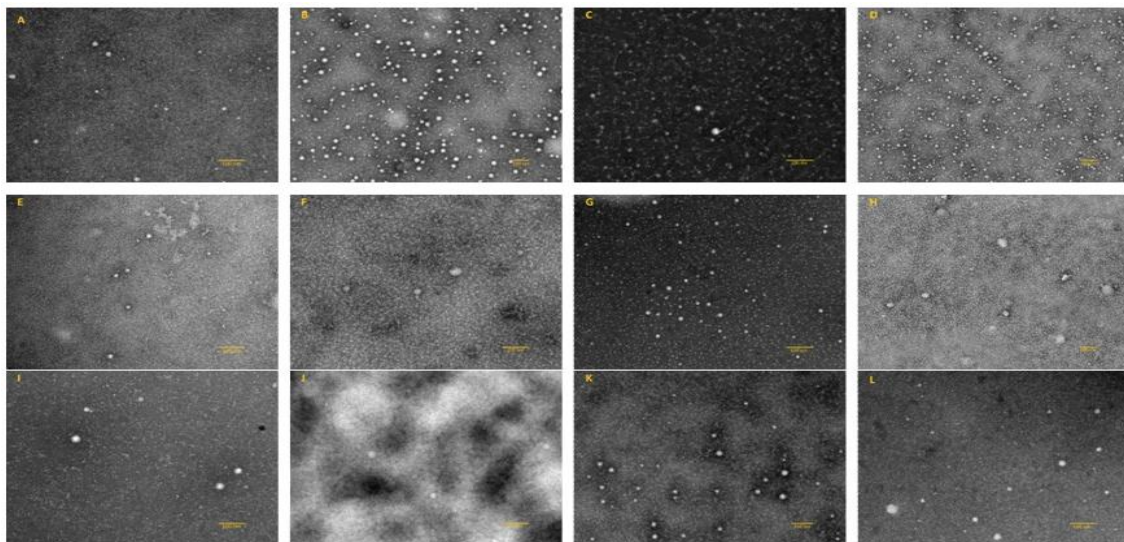


**Figure3.** Micrographs of electrostatically precipitated particles formed from alpha-lactalbumin at concentrations of 2 mg/L (A), 5 mg/L (B), 15 mg/L (C), 25 mg/L (D); soy protein isolate at concentrations of 2 mg/L (E), 5 mg/L (F), 15 mg/L (G), 25 mg/L (H); whey protein isolate at concentrations of 2 mg/L (I), 5 mg/L (J), 15 mg/L (K), 25 mg/L (L).

**Relaxation times slope ( $\lambda$ ) and critical frequency value (CFV)**

Relaxation times slopes were similar ( $P > 0.05$ ) and ranged from -0.871 to -1.319, confirming that all the geometric structures were similar (Table 3). This observation was supported by the micrographs (the next section).

In this study, the CFV of the tested solutions ranged from 62.83 to 135.34 rad/s (Table 3), depending on the type of protein and the concentration. Higher concentrations of PSP-CAN yielded lower CFVs and this trend was more significant ( $P < 0.05$ ) for the WPI samples,

suggesting smaller particles. At 25 mg/L anthocyanins concentration, all samples had the same lower value of CFV of 62.83rad/s, indicating a less stable structure.

The SPI compounds produced smaller structures at the 5-25 mg/L concentration levels (lower CFV values) which were also more sensitive to shear –i.e., frequency. These results agree with the lower ACN -protein ratios of these compounds, suggesting larger interactions between the protein and the PSP-CAN matrix during the entrapment which destabilizes the protein structure (L’hocine, Boye& Arcand, 2006; Lu et al., 2015).

**Table3.** Relaxation time ( $\lambda$ ) slope and Critical Frequency Value (CFV) for PSP- ACN -protein complexes determined from frequency sweep data at 23°C.

Protein type- CAN Concentration (mg/L) <sup>1</sup>	□ Slope*	CFV [rad/s]	R <sup>2</sup>
WPI-2	-0.908±0.025 <sup>a</sup>	135.34	0.783
WPI-5	-1.096±0.042 <sup>ab</sup>	135.34	0.784
WPI-15	-0.944±0.096 <sup>ab</sup>	92.24	0.875
WPI-25	-0.726±0.143 <sup>ab</sup>	62.83	0.877
α-L-2	-1.085±0.016 <sup>b</sup>	92.24	0.855
α-L-5	-1.102±0.178 <sup>ab</sup>	92.24	0.881
αL-15	-0.913±0.054 <sup>ab</sup>	92.24	0.828
α-L-25	-0.943±0.031 <sup>ab</sup>	42.81	0.804
SPI-2	-1.018±0.020 <sup>ab</sup>	92.24	0.998
SPI-5	-1.015±0.033 <sup>ab</sup>	62.83	0.992
SPI-15	-0.977±0.069 <sup>ab</sup>	62.83	0.959
SPI-25	-0.997±0.017 <sup>a</sup>	62.83	0.994

<sup>1</sup>WPI = Whey Protein Isolate; (α-L) = α-lactalbumin; SPI = Soy Protein Isolate , \*Values represent means ± standard deviation of three replicates per set of data, <sup>ab</sup>Mean values with a different superscript letter are significantly different than the others ( $p < 0.05$ ). LVR at 0.01 Pa for WPI and α-L samples and 0.1 Pa for SPI samples

**Morphology, Size and Distribution of PSP-ACN Particles**

Samples manufactured with α-L had larger anthocyanin particles with increasing concentrations, as they ranged from ~20nm to ~45nm for 2mg/L and 5mg/LPSP- ACN concentrations, respectively (Figures 3A and 3B). At higher concentrations (15 and 25 mg/L), no effect on the size of the particles was observed; however, the distribution changed and produced a more saturated image with a larger number of entrapped PSP-CAN particles, some of them clustered at the higher concentrations (Figures 3C and 3D). Similar results were found for the WPI and SPI samples where the size of PSP-ACN particles was not visually affected by the increase in the concentration of anthocyanins. However, SPI samples had smaller particle size (~12nm) in comparison to the samples from α-L and WPI (Figures 3E and 3G). The same conclusion was reached from the CFV data. The

distribution of PSP-ACN particles within the protein matrix at higher PSP-CAN concentration was different for SPI and WPI in comparison to α-L which displayed a smaller amount of PSP-CAN particles in the micrographs (Puerta-Gomez & Castell-Perez, 2016).

The morphology of PSP-CAN particles for all three protein matrices was characterized as being round and spherical in shape, except for the particles from the higher PSP-CAN concentrations in SPI, which looked like irregular ellipsoids that were larger in size. Again, this result agrees with the higher number of interactions between anthocyanins and the protein already characterized with the rheological analysis and ACN-protein ratio calculations.

In terms of their particle size distribution, samples prepared with SPI and α-L followed a similar trend (where the size of the compound was inversely proportional to the concentration

## Characterization of Protein-Based Complexes loaded with anthocyanins from Purple Sweet Potato

of PSP-ACN, thus resulting in samples with a smaller particle size). A different scenario was observed for WPI samples where the increase in PSP-ACN concentration resulted in a slight increase in particle size from 175.4 $\mu$ m to 208.6 $\mu$ m; this could be linked to the relaxation times “ $\lambda$ ”

of WPI where the trend of an increase in PSP-CAN concentration made an evident reduction in the CFV values, meaning that the increase in particle size lowers the breaking point of the structure along the frequency range, where changes in its 3D configuration can be perceived.

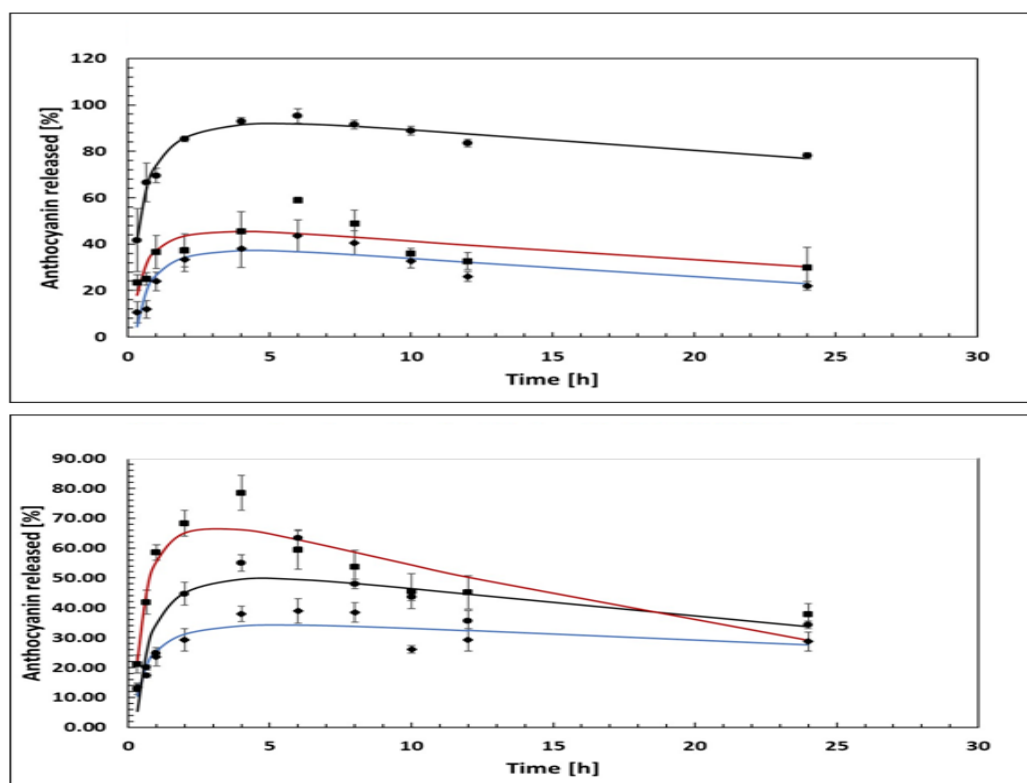


**Figure 4.** Percent release of PSP-ACN over 24 hours at 35°C. Top: pH = 1.35. Bottom: pH = 7.45 (□-L: WPI;○-L: SPI)

### In Vitro Release of Protein-Based Encapsulated PSP-ACN

The release profiles of anthocyanins from the protein matrices are shown in Fig. 4. Their release kinetics was best described by a second-order logarithmic model (Table 4). All SPI,  $\alpha$ -L and WPI samples showed similar release behavior with an initial rapid release then followed by a more constant release, with the exception of SPI at pH 7.45. Under acidic conditions (pH = 1.35), the  $\alpha$ -L samples released higher amounts of

ACN (85-90% after 4 hours) while the SPI samples released the least amount (40%) (Figure 4, top), mostly because the ACNs exhibit positive charges at low pH thus reducing the surface charges of the pH-sensitive protein below its isoelectric point (4.2- 4.5) and promoting the release of the active compound from the  $\alpha$ -L matrix (Lu et al., 2015). The WPI samples yielded a maximum release of 50%. Similar trends were found after 12 hours, with the highest amount of PSP-ACN released from the  $\alpha$ -L matrix.

**Table 4.** Second-order logarithmic model describing the kinetics of release of PSP-ACN under pH = 1.35 and pH = 7.45

pH = 1.35	a	b	c	R <sup>2</sup>	SE
WPI <sup>1</sup>	37.20	12.26	-4.55	0.780	7.81
$\alpha$ -L	73.87	21.80	-6.55	0.810	2.89
SPI	26.48	14.45	-4.90	0.990	5.62
pH = 7.45	a	b	c	R <sup>2</sup>	SE
WPI	55.49	20.11	-8.94	0.910	7.58
$\alpha$ -L	34.53	19.41	-6.19	0.890	8.36
SPI	25.55	10.32	-3.05	0.910	4.58

1WPI = Whey Protein Isolate; ( $\alpha$ -L) =  $\alpha$ -lactalbumin; SPI = Soy Protein Isolate, a, b and c are model parameters (Eq. 8); R<sup>2</sup> = coefficient of determination; SE = standard error

At pH = 7.45, the SPI and  $\alpha$ -L displayed slower release rates (Figure 4, bottom). The smaller percent release of PSP-ACN at higher pH is explained by the electrostatic interaction between the capsules and anthocyanins being strongest at the higher pH, and the drastic decrease in the charge density of anthocyanins at the lower pH (Fernandes, de Freitas & Mateus, 2014).

The WPI samples released the entrapped anthocyanin earlier and at the highest level, reaching 78% and 55% after 4 and 12 hours, respectively; next followed the  $\alpha$ -L samples with 50% and 35% after 4 and 12 hours, respectively. SPI samples maintained a constant trend of percent release between the 4- and 12-hours interval (26%). These results are supported by the more gel-like SPI complexes which make entrapment more difficult with lower %EE%, %LC, and PSP-ACN-protein ratios as described before. Similar trends have been found with other compounds and matrices (Oidtmann et al., 2012; Chien, Chung & Shah, 2014).

### CONCLUSIONS

The mechanical spectra of the tested PSP-ACN-protein compounds provided new knowledge on the structure and stability of the compounds during processing (e.g., shearing rates during injection or other applications inducing shear rates).

The Viscoelastic characteristics of the diluted polymeric solutions correlated well with the entrapment efficiency (%EE) and loading capacity (%LC) results with the more solid-like compounds being less effective. Transmission electron microscopy of the electrostatically precipitated proteins confirmed that relaxation time slope and CFV values relate well to the shape, size and shear stability of the assembled structures. Release studies showed that both WPI and  $\alpha$ -L matrices are viable options to offer immediate protection of the PSP- CAN while retarding the release of the entrapped antioxidant compound within a 6 - 12 hour time frame.

In brief, correlations among %EE, TEM, particle size analysis, release profile and rheological characteristics of the polymeric dilute solutions suggest that WPI and  $\alpha$ -L matrices are the most suitable candidates for development of carriers of the antioxidant evaluated in this study. Future work will include stability studies of developed carriers during steaming, drying and other processing of fortified foods.

### ACKNOWLEDGEMENTS

The authors thank Dr. Chad Mashuga from the Chemical Engineering Department and Dr. Ross Payne from the Department of Veterinary Medicine and Biomedical Sciences at Texas A&M University (College Station, TX) for their technical assistance and use of their lab facilities and equipment for particle size analysis and microscopic evaluations.

### AUTHOR CONTRIBUTIONS

Mauricio Martinon and Zeynep Sevimli-Yurttas carried out the experiments and conducted data analysis. Zeynep Sevimli-Yurttas helped with experiments and data analysis. Rosana Moreira supervised the development of the experimental plans and helped with data analysis. Elena Castell-Perez developed the concept and objectives of the study, supervised rheological experiments, assisted with data analysis and drafted the manuscript. She is the corresponding author.

### CONFLICT OF INTEREST

There is no conflict of interest to declare.

### REFERENCES

- [1] Ahmed, M., Akter, M.S., Lee, J.C. & Eun, J. (2010). Encapsulation by spray drying of bioactive components, physicochemical and morphological properties from purple sweet potato. *LWT-Food Science and Technology* 43(9), 1307-1312.
- [2] Bovell-Benjamin, A.C. (2007). Sweet potato: A review of its past, present, and future role in human nutrition. *Advances in Food and Nutrition Research*, 52, 1-59.
- [3] Bridgers, E. N., Chin, M. S., & Van-den, T. (2010). Extraction of anthocyanins from industrial purple fleshed sweet potatoes and enzymatic hydrolysis of residues from fermentable sugars. *Industrial Crops and Products*, 32, 613-620.
- [4] Chamberlain, E.K., Rao, M.A., (2000). Effect of concentration on rheological properties of acid-hydrolyzed amylopectin in solutions. *Food Hydrocolloids* 14(2), 163-171.
- [5] Chien, K. B., Chung, E. J., & Shah, R.N. (2014). Investigation of soy protein hydrogels for biomedical applications: Materials characterization, drug release, and biocompatibility. *Journal of Biomaterials Applications*, 28(7) 1085-1096.
- [6] Crowe, K.M. (2013). Designing Functional Foods with Bioactive Polyphenols: Highlighting Lessons Learned from Original Plant Matrices. *Journal of Human Nutrition & Food Science*, 1(3), 1018.

- [7] Fernandes, I., de Freitas, V., & Mateus, N. (2014). Anthocyanins and human health: How gastric absorption may influence acute human physiology. *Nutrition and Aging*, 2, 1-14.
- [8] Garti, N. (2008). *Delivery and Controlled Release of Bioactives in Foods and Nutraceuticals*. Woodhead Publishing, Boca Raton, FL.
- [9] Giusti, M.M., & Wrolstad, R.E. (2001). *Characterization and Measurement of Anthocyanins by UV-Visible Spectroscopy, Current Protocols in Food Analytical Chemistry*. John Wiley & Sons, Inc., pp. F1.2.1-F1.2.18.
- [10] Gunasekaran, S., Ko, S., & Xiao, L. (2007). Use of whey proteins for encapsulation and controlled delivery applications. *Journal of Food Engineering*, 83(1), 31-40.
- [11] He, J. & Giusti, M.M. (2010). Anthocyanins: natural colorants with health-promoting properties. *Annual Reviews Food Science and Technology*, 1, 163-187.
- [12] Kamonpatana, K., Giusti, M.M., Chitchumroon chokchai, C., M cruz, M.M., Riedl, K.M., Kumar, P., & Failla, M.L. (2012). Susceptibility of anthocyanins to *ex vivo* degradation in human saliva. *Food Chemistry*, 135, 738-747.
- [13] Li, A., Xiao, R., He, S., An, X., He, Y., Wang, C., Yin, S., Wang, B., Shi, X., & He, J. (2019). Research advances of purple sweet potato anthocyanins: extraction, identification, stability, bioactivity, application, and biotransformation. A review. *Molecules* 24, 3816-837.
- [14] Liu, X. Y., Zhang, D., Wu, Y.P., Wang, D., Wei, Y., Wu, J. & Ji, B. (2014). Stability and absorption of anthocyanins from blueberries subjected to a simulated digestion process. *International Journal of Food Science and Nutrition*, 65(4), 440-448.
- [15] L'hocine, L., Boye, J.I. & Arcand, Y. (2006). Composition and functional properties of soy protein isolates prepared using alternative defatting and extraction procedures. *AGRI* (193), C137-C145.
- [16] Lu, M., Li, Z., Liang, H., Shi, M., Zhao, L., Li, W., Chen, Y., Wu, J., Wang, S., Chen, X., Yuan, Q. & Li, Y. (2015). Controlled release of anthocyanins from oxidized konjac glucomannan microspheres stabilized by chitosan oligosaccharides. *Food Hydrocolloids*, 51, 476-485.
- [17] Oidtmann, J., Schantz, M., Maeder, K., Baum, M., Berg, S., Betz, M., Kulozik, U., Leick, S., Rehage, H., Schwarz, K. & Richling, E. (2012). Preparation and comparative release characteristics of three anthocyanin encapsulation systems. *Journal of Agricultural and Food Chemistry*, 60(3), 844-851.
- [18] Osaki, K., Inoue, T., & Uematsu, T. (2001). Viscoelastic properties of dilute polymer solutions: The effect of varying the concentration. *J. Poly. Sci. Part B: Polymer Physics*, 1, 39(2), 211-217.
- [19] Pacheco-Palencia, L.A., Hawken, P., & Talcott, S.T. (2007). Juice matrix composition and ascorbic acid fortification effects on the phytochemical, antioxidant, and pigment stability of açai (*Euterpe oleracea* Mart.). *Food Chemistry*, 105, 28-35.
- [20] Padzil, A., Aziz, A., & Muhamad, I.I. (2019). Physicochemical properties of encapsulated purple sweet potato extract; effect of maltodextrin concentration, and microwave drying power. *Malaysian Journal of Analytical Sciences* 22(4), 612-618.
- [21] Parada, J., & Aguilera, J.M. (2007). Food microstructure affects the bioavailability of several nutrients. *Journal of Food Science*, 72(2), R21-R32.
- [22] Peng, Z., Li, J., Guan, Y., & Zhao, G. (2013). Effect of carriers on physicochemical properties, antioxidant activities and biological components of spray-dried purple sweet potato flours. *LWT- Food Science and technology* 51(1): 348-355.
- [23] Pojer, E., Mattivi, F., Johnson, D. & Stockley, C.S. (2013). The case for anthocyanin consumption to promote human health: a review. *Comprehensive Reviews Food Science and Food Safety*, 12, 83-508.
- [24] Puerta-Gomez, A.F. & Castell-Perez, M.E. (2015). Physical Stability of Octenyl Succinate-Modified Polysaccharides and Whey Proteins for Potential Use as Bioactive Carriers in Food Systems. *Journal of Food Science*, 80(6), E1209-E1217.
- [25] Puerta-Gomez, A.F. & Castell-Perez, M.E. (2016). Studies in self-assembly interactions of proteins and octenyl succinic anhydride (OSA)-modified depolymerized waxy rice starch using rheological principles. *Journal of Applied Polymer Science*, 43603, 11 pages.
- [26] Ray, R.C., Panda, S.K., Swain, M.R., & Sivakumar, P.S. (2012). Proximate composition and sensory evaluation of anthocyanin-rich purple sweet potato (*Ipomoea batatas* L.) wine. *International Journal of Food Science and Technology*, 47:452-8.
- [27] Ribnicky, D.M.; Roopchand, D.E.; Oren, A.; Grace, M.; Poulev, A.; Lila, M.A.; Havenaar, R.; & Raskin, I. (2014). Effects of a high fat meal matrix and protein complexation on the bioaccessibility of blueberry anthocyanins using the TNO gastrointestinal model (TIM-1). *Food Chemistry*, 349-357.
- [28] Roland, C. (2008). Characteristic relaxation times and their invariance to thermodynamic conditions. *Soft Matter*, 12, 2316- 2322.
- [29] Schramm, G. A. (2002). *Practical Approach to Rheology and Rheometry*, 2nd ed.; Thermo Haake GmbH: Karlsruhe, Germany.

## Characterization of Protein-Based Complexes loaded with anthocyanins from Purple Sweet Potato

- [30] Sunthar, P., (2010). Polymer Rheology, in: Krishnan, J.M., Deshpande, A.P., Kumar, P.B.S. (Eds.), *Rheology of Complex Fluids*. Springer New York, pp. 171-191.
- [31] Sigma Plot. (2019). Version V1.7. Systat Software, Inc. San Jose, California.
- [32] Suda, I., Ishikawa, F., Hatakeyama, M., Miyawaki, M., Kudo, T., Hirano, K., Ito, A., Yamakawa, O. & Horiuchi, S.(2008). Intake of purple sweet potato beverage effects on serum hepatic biomarker levels of healthy adult men with borderline hepatitis. *European Journal of Clinical Nutrition*, 62:60–7.
- [33] Utracki, L.A., (2004). Clay-containing Polymeric Nano composites, *Technology & Engineering*. iSmithersRapra Publishing, pp. 27-54.
- [34] Woodward, G., Kroon, P., Cassidy, A. & Kay, C. (2009). Anthocyanin stability and recovery: implications for the analysis of clinical and experimental samples. *Journal of Agricultural and Food Chemistry*, 57912, 5271-5278.
- [35] Wrolstad, R. E. (2002). *Current protocols in food analytical chemistry*. (pp. F1.2.1 – F1.2.6). New York: John Wiley.

**Citation:** M. Elena Castell-Perez, Mauricio E. Martinon, Zeynep Sevimli-Yurttas, Rosana G. Moreira, "Characterization of Protein-Based Complexes loaded with anthocyanins from Purple Sweet Potato", *Research Journal of Food and Nutrition*, 3(3), 2019, pp. 22-32.

**Copyright:** © 2019 M. Elena Castell-Perez, This is an open-access article distributed under the terms of the Creative Commons Attribution License, which permits unrestricted use, distribution, and reproduction in any medium, provided the original author and source are credited.